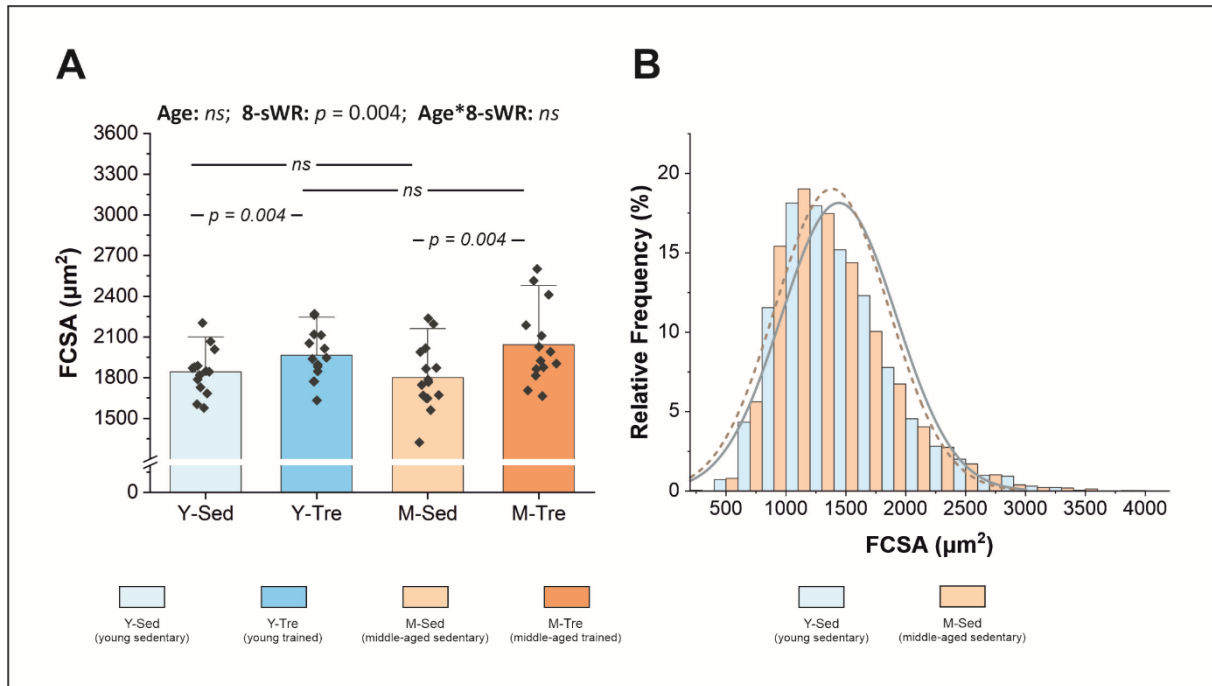


Physical activity reverses the aging induced decline in angiogenic potential in the fast locomotory muscles of mice

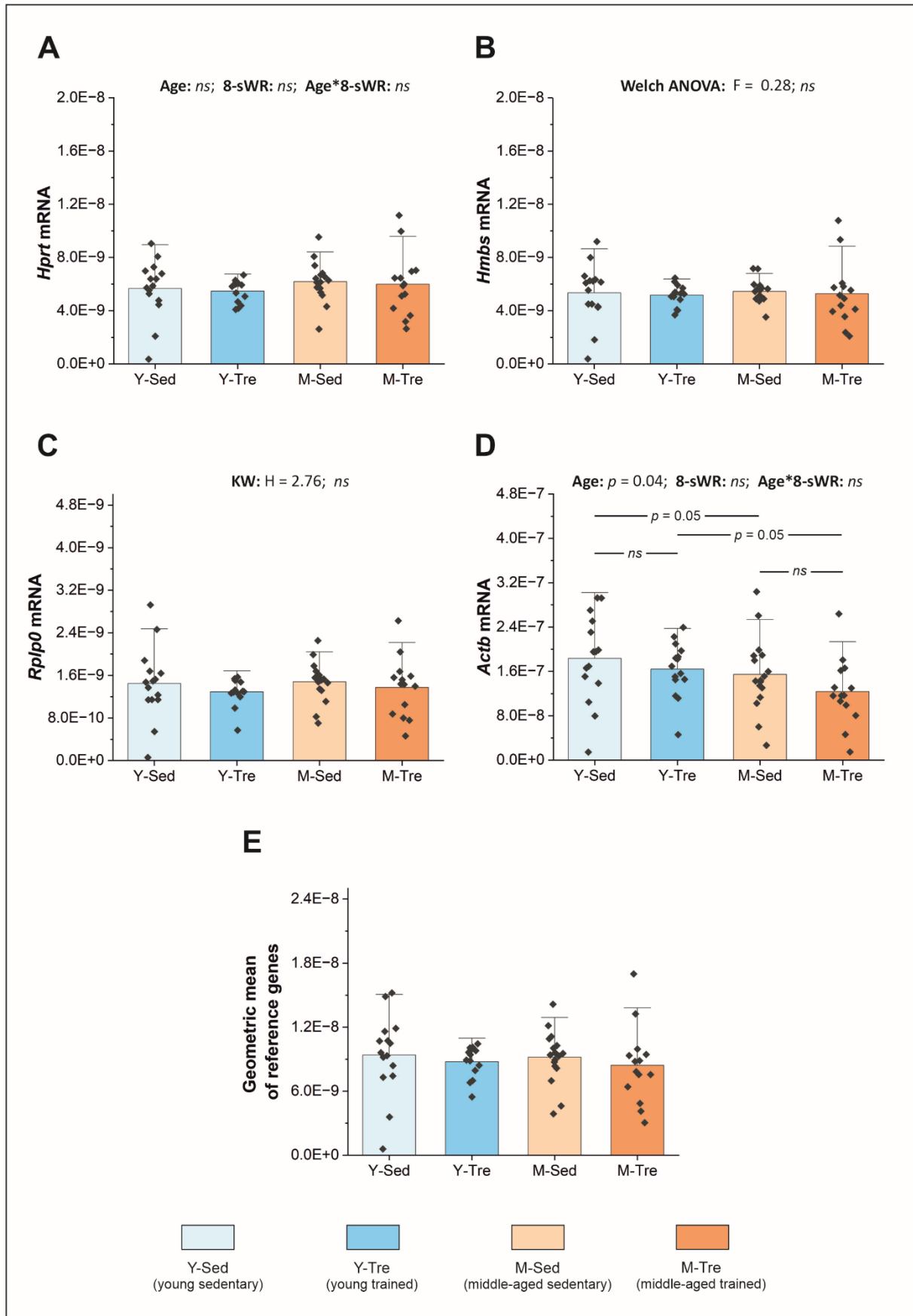
Magdalena Zmudzka^{1#}, Joanna Szramel^{1#}, Janusz Karasinski², Zenon Nieckarz³,
Jerzy A. Zoladz¹, Joanna Majerczak¹

Supplemental Figure S1



Supplemental Figure S1. Fiber cross-sectional area (FCSA) of the fast-twitch tibialis anterior (TA) muscle. FCSA in the TA muscle of the sedentary and trained groups of young (Y) and middle-aged (M) mice ($n = 14-14-15-14$) (**A**). The data are presented as the means + SDs. Each data point in the dot plot represents a mean value of the FCSA measured for each mouse. Two-way ANOVA followed by Tukey's *post hoc* test was used. Statistically significant changes ($p < 0.05$) are plotted on the graphs; *ns*, not statistically significant. Distribution of the FCSA in the TA muscle of young sedentary and middle-aged sedentary groups of mice (on the basis of the 3186 vs 3632 FCSA results, respectively) (**B**).

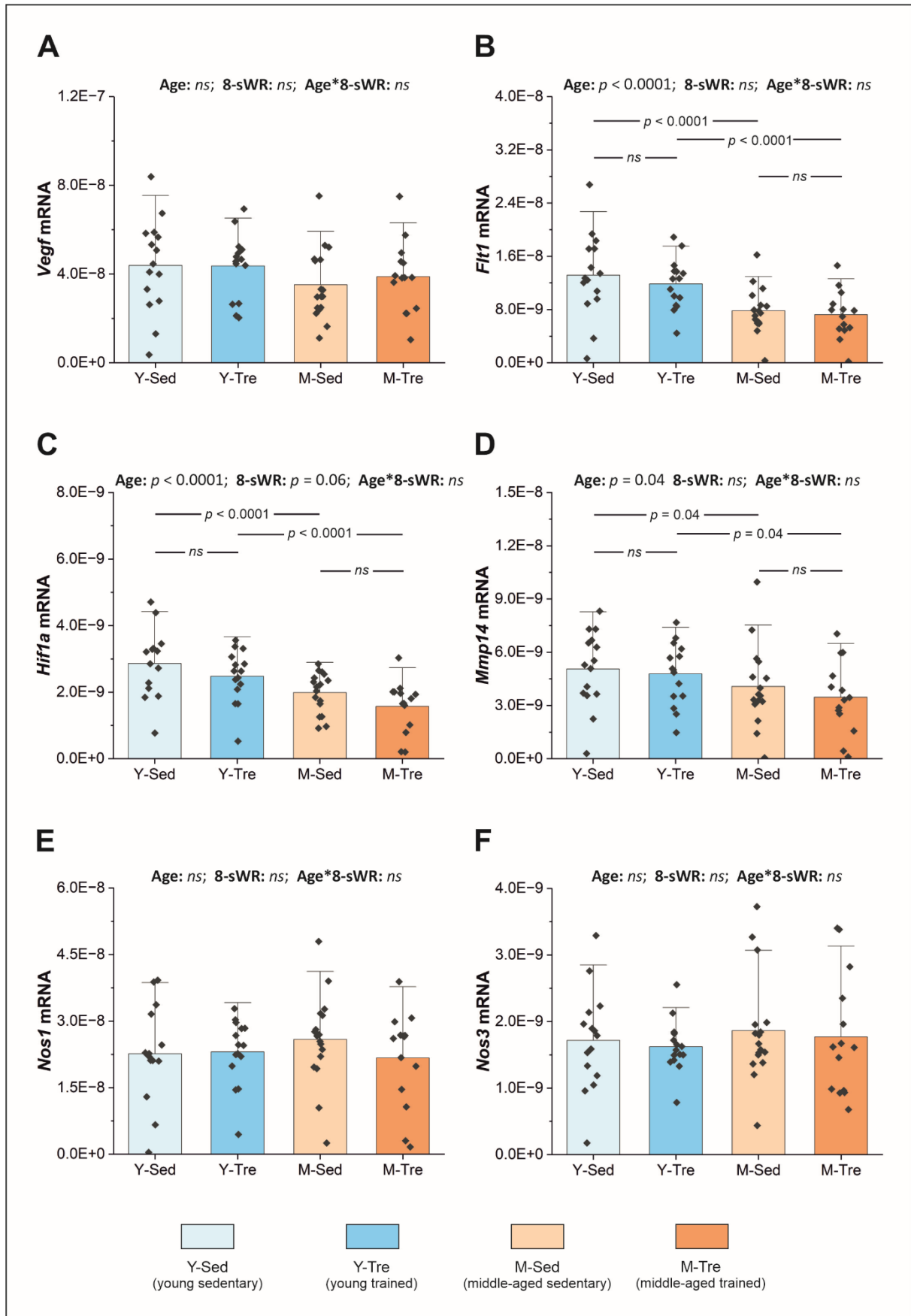
Supplemental Figure S2



Supplemental Figure S2. Reference gene expression in the fast-twitch extensor digitorum longus (EDL) muscle in the sedentary and trained groups of young (Y) and middle-aged (M) mice. The mRNA expression of hypoxanthine guanine phosphoribosyl transferase (*Hprt*) ($n = 15-14-17-14$) (A); hydroxymethylbilane

synthase (*Hmbs*) (n = 15–14–16–14) (**B**); ribosomal protein, large, P0 (*Rplp0*) (n = 15–14–17–14) (**C**); actin, beta (*Actb*) (n = 15–15–17–14) (**D**); and the geometric mean of all four analyzed reference genes, i.e., *Hprt*, *Hmbs*, *Rplp0*, *Actb* (n = 15–14–17–14) (**E**). The data are presented as the means + SDs. Each data point in the dot plot represents one individual mouse sample. Two-way ANOVA followed by Tukey's *post hoc* test (**A**, **D** and **E**), Welch ANOVA followed by a Games–Howell *post hoc* test (**B**) and the Kruskal–Wallis (KW) test followed by Dunn's *post hoc* test were used (**C**). Statistically significant changes ($p < 0.05$) are plotted on the graphs; *ns*, not statistically significant.

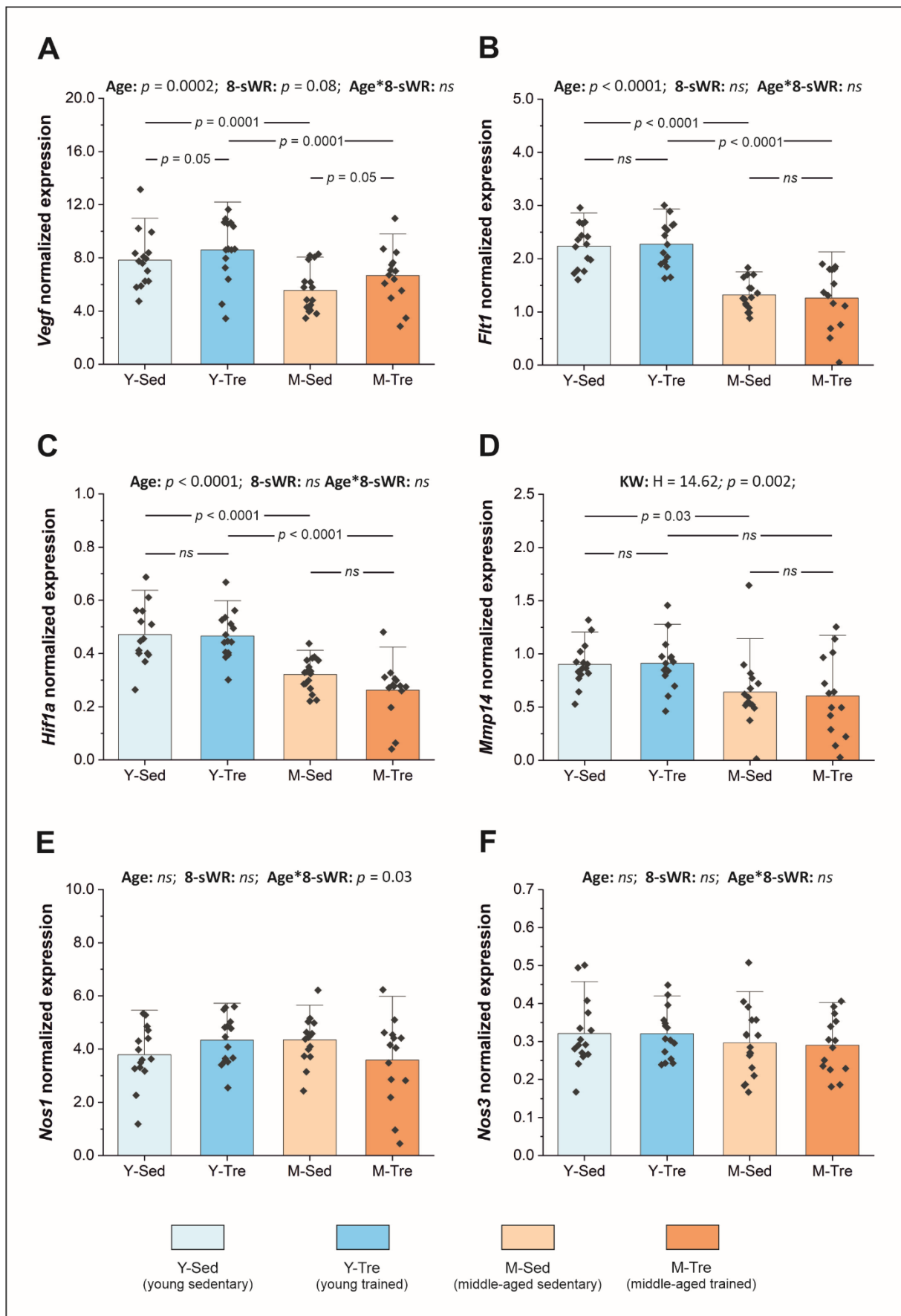
Supplemental Figure S3



Supplemental Figure S3. Pro-angiogenic genes expression (raw data) in the fast-twitch extensor digitorum longus (EDL) muscle in the sedentary and trained groups of young (Y) and middle-aged (M) mice. The mRNA expression of vascular endothelial growth factor A (*Vegfa*) (n = 15–15–17–14) (A); FMS-like tyrosine

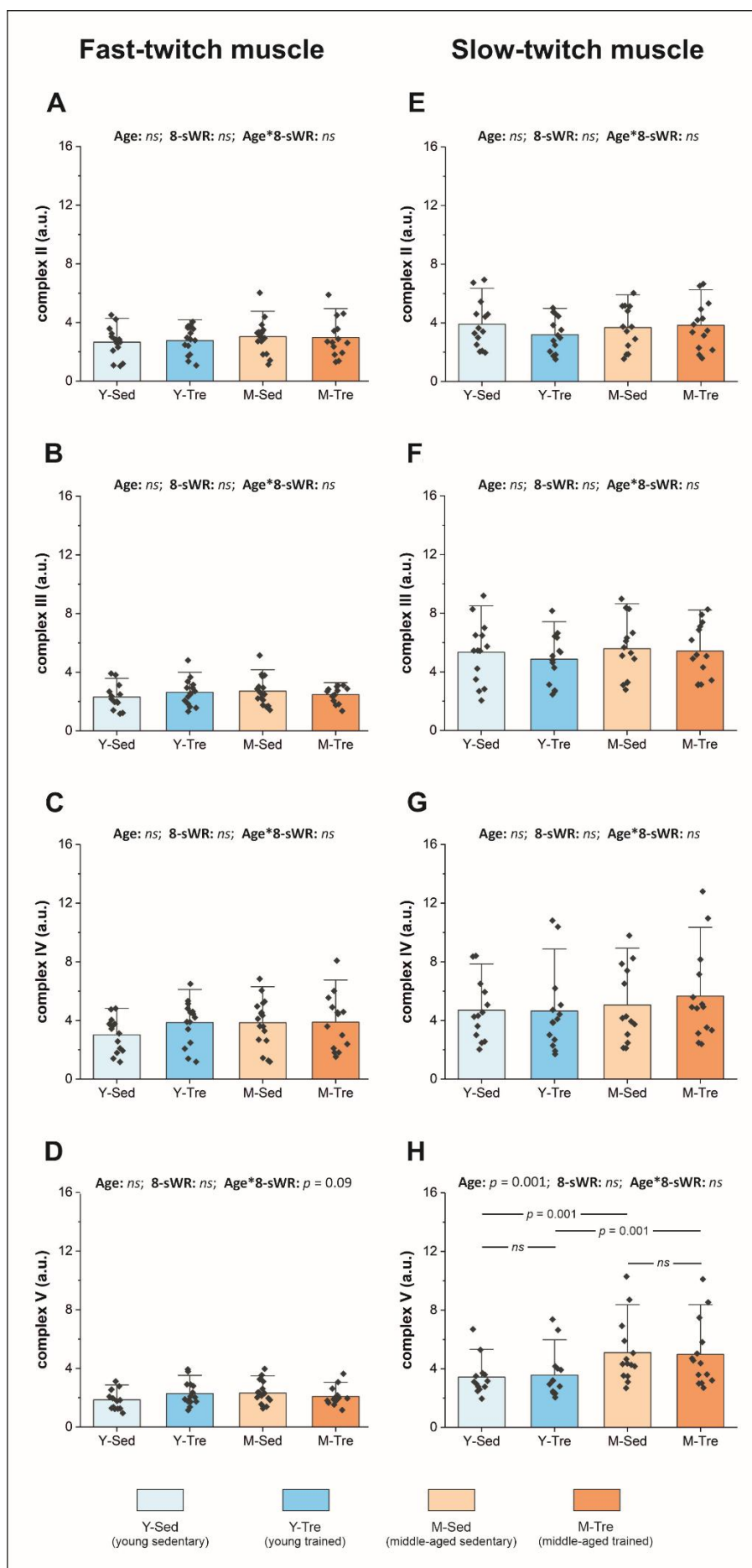
kinase 1 (*Flt1*) (n = 15–15–17–14) (**B**); hypoxia-inducible factor 1, alpha subunit (*Hif1a*) (n = 14–15–17–14) (**C**); matrix metalloproteinase 14 (*Mmp14*) (n = 15–15–16–14) (**D**); nitric oxide synthase 1 (*Nos1*) (n = 15–15–17–14) (**E**); nitric oxide synthase 3 (*Nos3*) (n = 15–15–17–14) (**F**). The data are presented as the means + SDs. Each data point in the dot plot represents one individual mouse sample. Two-way ANOVA followed by Tukey's *post hoc* test was used. Statistically significant changes ($p < 0.05$) are plotted on the graphs; *ns*, not statistically significant.

Supplemental Figure S4



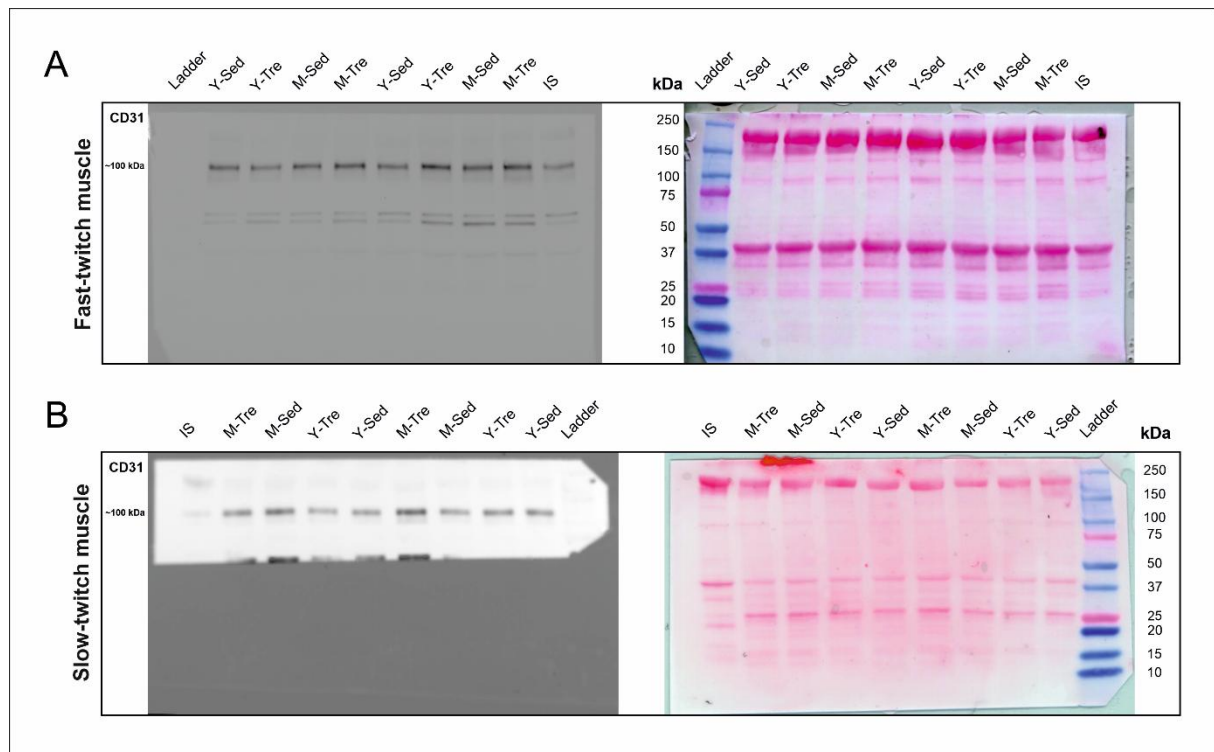
Supplemental Figure S4. Pro-angiogenic genes expression (normalized to *Hprt*) in the fast-twitch extensor digitorum longus (EDL) muscle in the sedentary and trained groups of young (Y) and middle-aged (M) mice. The expression of vascular endothelial growth factor A (*Vegfa*) (n = 15–15–17–14) (**A**); FMS-like tyrosine kinase 1 (*Flt1*) (n = 15–15–16–14) (**B**); hypoxia-inducible factor 1, alpha subunit (*Hif1a*) (n = 14–15–17–14) (**C**); matrix metalloproteinase 14 (*Mmp14*) (n = 15–15–16–14) (**D**); nitric oxide synthase 1 (*Nos1*) (n = 15–15–16–14) (**E**); nitric oxide synthase 3 (*Nos3*) (n = 15–15–17–14) (**F**). The data are presented as the means + SDs. Each data point in the dot plot represents one individual mouse sample. Two-way ANOVA followed by Tukey's *post hoc* test (**A–C, E and F**) and the Kruskal–Wallis (KW) test followed by Dunn's *post hoc* test were used (**D**). Statistically significant changes ($p < 0.05$) are plotted on the graphs; *ns*, not statistically significant.

Supplemental Figure S5



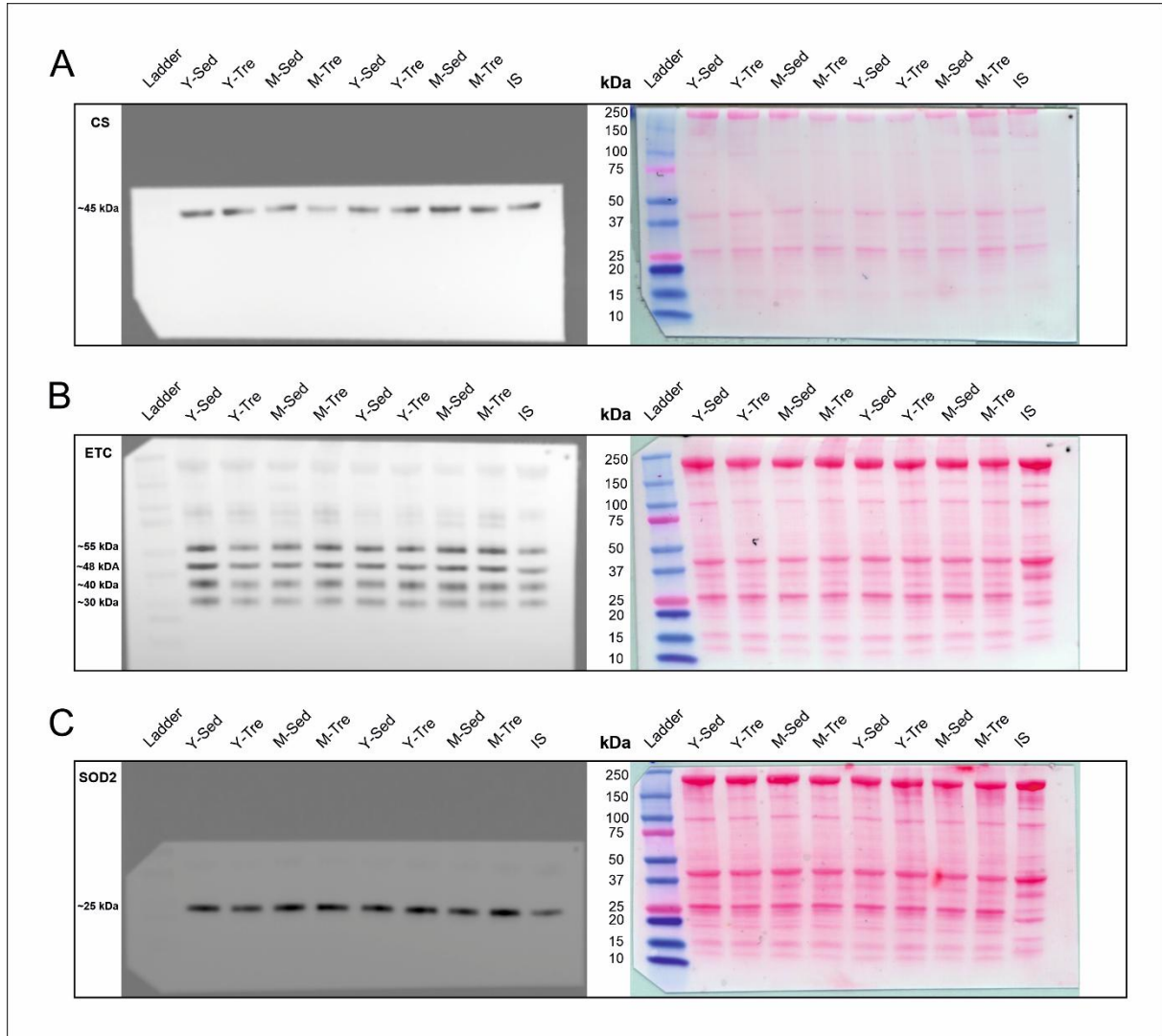
Supplemental Figure S5. Electron transport chain (ETC) proteins in the fast-twitch tibialis anterior (TA) and slow-twitch soleus (Sol) muscles in the sedentary and trained groups of young (Y) and middle-aged (M) mice. The contents of complex II (n = 14–15–17–14) (A), complex III (n = 14–15–17–14) (B), complex IV (n = 14–15–17–14) (C), and complex V (n = 14–15–17–14) (D) in the TA muscle. The contents of complex II (n = 14–14–13–14) (E), complex III (n = 14–14–14–14) (F), complex IV (n = 13–14–13–14) (G), and complex V (n = 13–14–14–14) (H) in the Sol muscle. The data are presented as the means + SDs. Each data point in the dot plot represents one individual mouse sample. Two-way ANOVA with repeated measures followed by Tukey's *post hoc* test was used. Statistically significant changes ($p < 0.05$) are plotted on the graphs; *ns*, not statistically significant.

Supplemental Figure S6



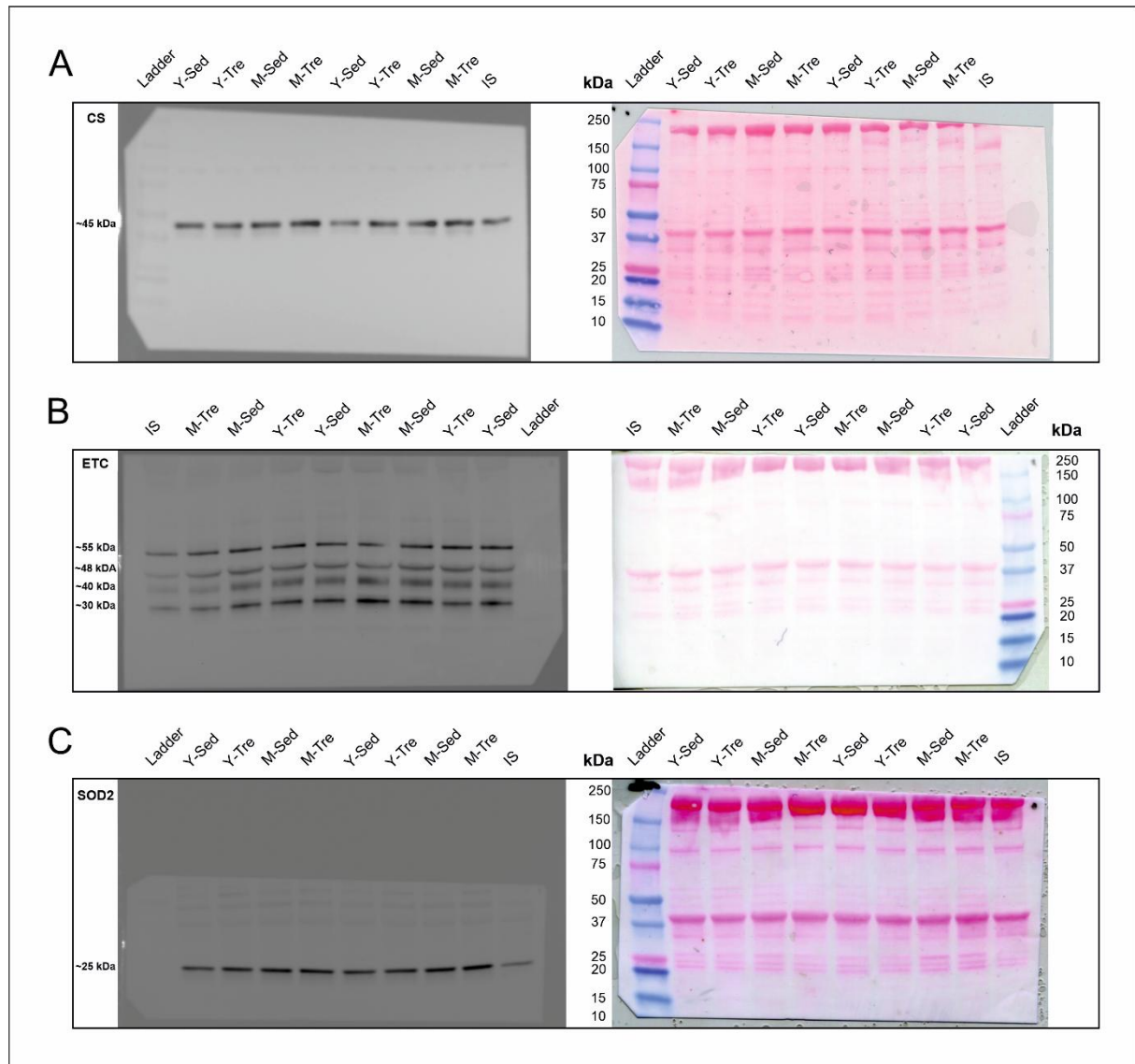
Supplemental Figure S6. Representative immunoblots demonstrating the detection of platelet endothelial cell adhesion molecule (CD31) protein in the fast-twitch tibialis anterior (TA) and slow-twitch soleus (Sol) muscles in sedentary and trained groups of young (Y) and middle-aged (M) mice. CD31 content in the TA (A) and Sol muscles (B). Ponceau S staining (right side) of the same membranes demonstrating total protein loaded. The protein ladder is a visible Precision Plus Protein Dual Color Standards (Bio-Rad, Cat# 1610374). The internal standard (IS) was a gastrocnemius sample from a wild-type mouse. **Abbreviations:** Y-Sed, young sedentary; Y-Tre, young trained; M-Sed, middle-aged sedentary; M-Tre, middle-aged trained.

Supplemental Figure S7



Supplemental Figure S7. Representative immunoblots showing the detection of mitochondrial protein expression in the fast-twitch tibialis anterior (TA) muscle in the sedentary and trained groups of young (Y) and middle-aged (M) mice. Citrate synthase content (CS) (~45 kDa) (**A**). The electron transport chain (ETC) protein contents including: complex II (~55 kDa), complex III (~48 kDa), complex IV (~40 kDa), and complex V (~30 kDa) (**B**). SOD2 content (~25 kDa) (**C**). Ponceau S staining (right side) of the same membranes demonstrating total protein loaded. The protein ladder is a visible Precision Plus Protein Dual Color Standards (Bio-Rad, Cat# 1610374). The internal standard (IS) was a gastrocnemius sample from a wild-type mouse. **Abbreviations:** Y-Sed, young sedentary; Y-Tre, young trained; M-Sed, middle-aged sedentary; M-Tre, middle-aged trained.

Supplemental Figure S8



Supplemental Figure S8. Representative immunoblots demonstrating showing the detection of mitochondrial protein expression in the slow-twitch soleus (Sol) muscle in the sedentary and trained groups of young (Y) and middle-aged (M) mice. Citrate synthase content (CS) (~45 kDa) (**A**). The electron transport chain (ETC) protein contents including: complex II (~55 kDa), complex III (~48 kDa), complex IV (~40 kDa), complex V (~30 kDa) (**B**). SOD2 content (~25 kDa) (**C**). Ponceau S staining (right side) of the same membranes demonstrating total protein loaded. The protein ladder is a visible Precision Plus Protein Dual Color Standards (Bio-Rad, Cat# 1610374). The internal standard (IS) was a mouse soleus (**A**) or gastrocnemius (**B** and **C**) sample from a wild-type mouse. **Abbreviations:** Y-Sed, young sedentary; Y-Tre, young trained; M-Sed, middle-aged sedentary; M-Tre, middle-aged trained.